Mj. Int. J. Sci. Tech. **2008**, *2*(01), 240-254

Maejo International
Journal of Science and Technology
ISSN 1905-7873
Available online at www.mijst.mju.ac.th

Full Paper

Computational analysis and visualisation of wind-driven naturally ventilated flows around a school building

Chanawat Nitatwichit*, Yottana Khunatorn, and Nakorn Tippayawong

Department of Mechanical Engineering, Faculty of Engineering, Chiang Mai University, Chiang Mai 50200, Thailand

* Author to whom correspondence should be addressed, e-mail: n_chanawat@mju.ac.th

Received: 4 December 2007 / Accepted: 14 March 2008 / Published: 22 March 2008

Abstract: Most Thai state schools are designed to use cross-flow natural ventilation as a passive cooling system. The aim of this study is to investigate the effects of geometry and orientation of a school building on the airflow distribution around it. Computational fluid dynamics (CFD) commercial software was used as a tool in this simulation. The 3-D flow simulation of the building domain was performed with prevailing wind to identify a proper strategy of flows around the building. It was found that the cross orientation of the building to wind direction might not necessarily result in good ventilation in classrooms. Flow visualisation with hydrogen bubble technique was set up to qualitatively validate the numerical results. A water flow was maintained at 3.7 cm/s, with corresponding to flow Reynolds number of 3,556. The numerical results were found to agree well with the experimental results.

Keywords: natural ventilation, CFD, school building, flow visualisation, hydrogen bubble technique

---

Introduction

There are approximately 350,000 schoolchildren in about 500 schools in densely populated communities such as municipalities and urban areas in Thailand. The majority of these schools are state-owned wherein most classrooms are naturally ventilated through open doors and windows. Air movement is allowed to penetrate the school buildings. At least 11 buildings of the state schools under

Chiang Mai municipality are constructed in standard dimensions according to the Ministry of Education. These four-storey school buildings have three classrooms, an activity room and a toilet in each of the floors except the ground floor, which is open space with no wall. The indoor air distribution is of great importance to students in the classroom. Poor indoor air quality in the classroom due to insufficient ventilation affects the students directly.

Ventilation is of three types, i.e. natural ventilation, mechanical ventilation and hybrid ventilation. The first type is increasingly becoming an important target for the design strategy to reduce the energy consumed by the air conditioning system with consequent reduction in CO_2 emission. Natural ventilation has been used as a powerful passive cooling method, especially in tropical regions like Thailand. Its advantage is the reduction of initial construction cost and operating cost for residential buildings while maintaining a ventilation rate consistent with the requirement of acceptable indoor air quality [1]. It can also improve indoor air quality, supply a high level of thermal comfort, and encourage energy saving on the air conditioning system. Two major types of natural ventilation are single-sided and cross ventilation. The former takes place when the building communicates with the outdoor environment through openings which are on the same exterior wall while the latter is mainly for naturally ventilated buildings. Normally the ventilation rate of a building is dependent on the wind and the temperature acting simultaneously. The pressure difference across an opening is defined as a function of two major forces, namely inertia and buoyancy. This is because indoor airflow patterns do not only depend on wind speed but also on the position and orientation of the building as well as the type, size, and position of the opening. Thus, a careful design of wind flow around a building is very important to fully utilise the potential of cross ventilation [2]. Changing of architectural design elements such as the position and orientation of the building, the roof shape, the balcony configuration type and the location of windows can modify the interior airflow magnitude and pattern. These architectural design elements govern the indoor airflow pattern and improve the indoor comfort level [3, 4].

A number of studies have been performed with a computational tool. Computational fluid dynamics (CFD) technique is an art of replacing the governing partial differential equations of fluid flow with numbers. It has become popular due to the fact that it supports and complements both pure experiment and pure theory, as well as its revealing results and low cost of labour and equipment. Particularly in the last two decades, the CFD technique was extensively used to predict the air movement within the rooms and around the buildings. Tantasvasdi et al. [5] explored the potential of using natural ventilation as a passive cooling system for new house designs in Thailand. CFD was used to calculate airflow in the house. It was found that it is preferable to have a larger inlet aperture than a larger outlet one. Sreshthaputra et al. [6] coupled energy simulation softwares, i.e. DOE-2 and CFD simulations to analyse heat transfer and airflow performance of an unconditioned 100-year-old Buddhist temple. Mochida et al. [7] investigated methods for controlling airflow in and around a building in order to improve indoor thermal comfort by utilising cross ventilation. Evola and Popov [8] applied CFD with Reynolds averaged Navier-Stokes equation (RANS) approach to wind-driven natural ventilation in a cubic building. Flows inside and around the cross and single-sided naturally ventilated buildings were determined. Like the CFD, flow visualisation has greatly assisted the fundamental understanding of a wide variety of fluid dynamic phenomena. A number of studies have been performed with the flow visualisation technique. Smith and Paxson [9] studied the motion and deformation of a hydrogen bubble time-line in time and space gathering digitally interfacing dual-view video sequences of a bubble time-line with a computer-aided display system. Latterly, Smith and Lu [10] used hydrogen-bubble flow visualisation pictures to establish local instantaneous velocity profile information. Eiamsa-ard et al. [11] studied experiments of the flow going past two obstacles near a channel wall using the hydrogen bubble technique. Bao and Dallmann [12] studied on the local separated flows around a rounded backward facing step using hydrogen bubble technique. Guo et al. [13] studied visually with conducting on the excited laminar-turbulent transition within a flat plate boundary layer flow in a water tunnel using hydrogen bubble technique. Zhang et al. [14] examined the aerodynamic characteristics of a square cylinder with an upstream rod in a staggered arrangement. Flow visualisation with hydrogen bubble technique was carried out.

The present research investigates the effects of building geometry and orientation on airflow distribution around a school building and in a typical state school classroom, which is designed as a cross-flow naturally ventilated room. CFDRC® [15], a commercial software, was used as a tool in this simulation by means of the finite volume method. A range of wind speeds and different wind directions, according to local meteorological conditions were utilised as the boundary conditions. Finally, flow visualisation with hydrogen bubble technique was used to verify the numerical results.

Materials and Methods

Numerical simulation

Wind flow patterns around building may strongly affect indoor air flow, thus investigating air flow around inlet openings of a classroom is important. The airflow pattern is predicted using a fundamental airflow model involving turbulence. A 3-D finite-volume approach is adopted by the software CFDRC® because of its capability of conserving solution quantities. The program solves the conservation equations for continuity, momentum, and energy as well as the equations for turbulent kinetic energy and its dissipation rate. The two-equation k - ε turbulence closure [16] is used. The governing equation of an incompressible steady-state flow can be written as

$$\nabla \bullet \left(\rho V \phi \right) = \nabla \bullet \left(\Gamma \nabla \phi \right) + S_{\phi} \tag{1}$$

where ρ is the air density, ϕ represents the mean velocity component, pressure and turbulent parameters, V is the mean velocity, Γ is the diffusion coefficient, and S_{ϕ} is the source term but it was ignored in this study. This equation is also known as the generic conservation equation for a quantity ϕ. Integrating this equation over a control-volume cell, we have

$$\int_{\vartheta} \nabla \bullet (\rho V \phi) d\vartheta = \int_{\vartheta} \nabla \bullet (\Gamma \nabla \phi) d\vartheta \tag{2}$$

In the k - ε turbulent model, the notation of k is the kinetic energy and ε is the turbulence dissipation rate. The turbulent viscosity is expressed as

$$v_t = \frac{C_\mu k^2}{\varepsilon} \tag{3}$$

The transport equations for k and ε are

$$\frac{\partial}{\partial t}(\rho k) + \frac{\partial}{\partial x_j}(\rho u_j k) = \rho P - \rho\varepsilon + \frac{\partial}{\partial x_j}\left[(\mu + \frac{\mu_t}{\sigma_k})\frac{\partial k}{\partial x_j}\right] \tag{4}$$

$$\frac{\partial}{\partial t}(\rho\varepsilon) + \frac{\partial}{\partial x_j}(\rho u_j \varepsilon) = C_{\varepsilon_1}\frac{\rho P\varepsilon}{k} - C_{\varepsilon_2}\frac{\rho\varepsilon^2}{k} + \frac{\partial}{\partial x_j}\left[(\mu + \frac{\mu_t}{\sigma_\varepsilon})\frac{\partial\varepsilon}{\partial x_j}\right] \tag{5}$$

with production term P defined as

$$P = v_t\left(\frac{\partial u_i}{\partial x_j} + \frac{\partial u_j}{\partial x_i} - \frac{2}{3}\frac{\partial u_m}{\partial x_m}\delta_{ij}\right)\frac{\partial u_i}{\partial x_j} - \frac{2}{3}k\frac{\partial u_m}{\partial x_m} \tag{6}$$

In the above equations, v_t is the turbulent viscosity, ρ is the fluid density, u_i and u_j are the mean velocity components in the x_i and x_j directions respectively, μ and μ_t are the laminar and turbulent dynamic viscosities respectively, and δ_{ij} is Kronecker delta. The turbulence model constants used in equations 3-6 are $C_\mu = 0.09$, $C_{\varepsilon_1} = 1.44$, $C_{\varepsilon_2} = 1.92$, $\sigma_k = 1.0$, and $\sigma_\varepsilon = 1.3$. To ensure the reliability of the simulation, model verification was performed by comparison of numerical results with Laser Doppler Anemometry (LDA) measurement of indoor air flows in a model room by Posner et al. [17]. The comparative results of the numerical simulations and experimental data were found to be in good agreement [18].

Model geometry

The school model is based on standard dimensions of the real school building. Figure 1 shows details of the building geometry at the façade. The dimensions are of 15.0 m × 36.3 m × 16.7 m (width × length × height). The dimensional detail of the computational domain is sufficiently large to avoid disturbance of the air flow around building. Each storey of the building (2^{nd}–4^{th} floor) has a similar room arrangement, i.e. three classrooms, a recreational room and a toilet. Figure 2 illustrates a horizontal section of 3^{rd} floor. A, B and C are classrooms, D is the toilet, and E is the recreational room. Each classroom has two doors with a space opening above each door. A corridor is a common path to every room on the floor. There are four sliding windows on the exterior wall. Overhang slabs at the façade and rear are designed for shading from excessive solar heat gain. For simplification, the building model is assumed to be located on a plane with no other buildings in the vicinity. To investigate effects of wind incidence angle (WIA) on the outdoor air flow, the building is rotated counterclockwise from the north in this square domain as detailed in Figure 3.

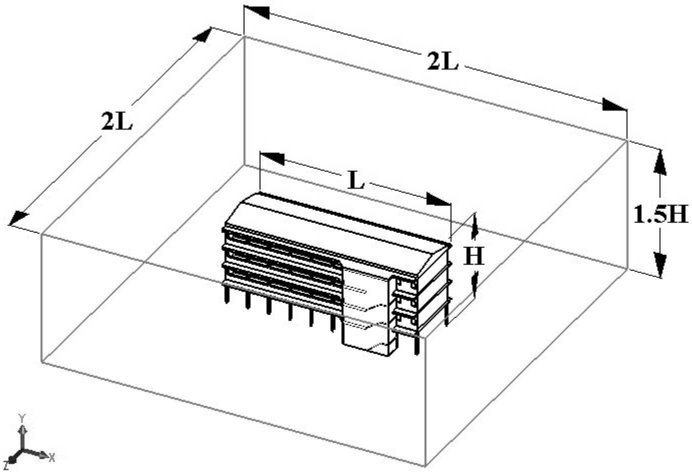

Figure 1. CFD model of school building

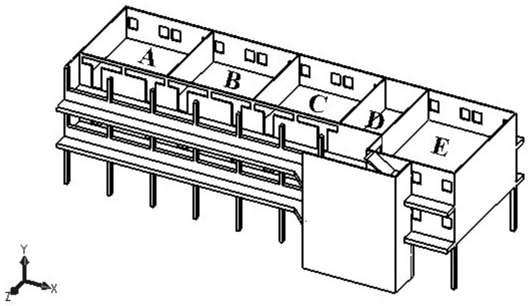

Figure 2. Typical sectional view of 3rd floor

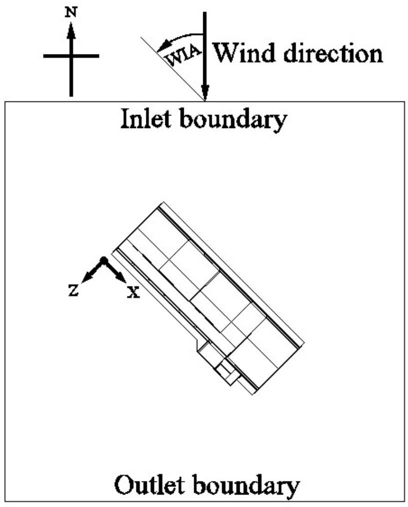

Figure 3. WIA with top view of building domain

Meshing

The computational domain has been changed by the building rotation within the domain. The tetrahedral cell has been chosen for meshing purpose. All computational domains of this study were undertaken for generating mesh by means of relative cell size. An actual mesh size was calculated by multiplying the length of the largest edge of the coordinate-aligned bounding box of the entity by a given parameter. The maximum relative cell size of 0.02 was used as a limit for generating local mesh of all domains. Meshing of this computational domain was carried out with 330,000 cells, covering the whole volume of the domain. A sensitivity analysis of the numerical scheme on the grid refinement was performed by using a finer grid, i.e. a relative cell size of 0.0175 (549,000 cells), but the change in the results was negligible. The simulations were carried out using the relative cell size of 0.02 because less time was required for solution convergence.

Model set-up and boundary conditions

The flow domain of the building was simulated with prevailing wind blowing along x-axis (Figure 1). Simulation of the real conditions is rather complicated due to the uncontrollable nature of the outdoor conditions. To reduce the complexity of the simulation, buoyancy effects are neglected. At a wind speed of 4 m/s, the buoyancy effect was diminished as a result of the wind-driven force [21]. All surfaces of the building domain are considered as isothermal walls and the no-slip condition is set at these walls. To simplify this computation, the flow is assumed to be a steady, incompressible and turbulent flow. The prevailing wind was set to blow through the inlet boundary from the north (Figure 3). At the outlet boundary of the domain, a constant pressure is assumed. The flow at the walls and ceiling of the domain box is simulated as the inlet boundary condition except for the ground being as the no-slip condition. To investigate the effect of WIA, the building is rotated 360^{o} counterclockwise around the center of the domain box with a 15° increment. The inlet boundary conditions of the building domain are presented as follows:

$$\frac{u}{u_o} = \left(\frac{z}{z_o}\right)^{\alpha} \tag{7}$$

where u is the local wind speed at elevation z, u_o is the meteorological wind speed at the reference elevation z_o, α is the parameter that varies with the ground roughness and is selected as 0.22 for the suburban area. The reference speed u_o is set at 4.0 m/s at the elevation z_o = 10 m.

Computational configuration

The calculations were carried out on an Intel Pentium®4-3.0 GHz with RAM of 1.0 GB. A converged solution was defined as either that the criterion of residual values of less than 0.0001 for all dependent variables was met or when the number of iterations arrived at 5000. Under-relaxation was applied to stabilise the convergence. Most cases were ended by convergence solutions.

Flow visualisation

A setup of flow visualisation arrangement is shown in Figure 4. The experiment was conducted in a low-speed multipurpose water tunnel. The walls of the test section were made of acrylic plate so that they were transparent to light sources. The suitable velocity of water was 3.7 cm/s. The working section area was 15 cm × 20 cm (width × length) and the depth of water was kept at 3 cm, corresponding to the open channel flow Reynolds number of 3,556. There were two water containers: a major tank which contained a water circulating pump, and a minor tank which received discharge water from the circulating pump.

The experimental setup consisted of: (a) a flow visualisation table, which contained all components on a steel frame, (b) two water tanks consisting of the major tank as the main reservoir and the minor tank which supplied water flow to the test section area, (c) the test section area which controlled water flow for a uniform flow and was equipped with a 0.25 mm-diameter stainless wire and electrodes to generate hydrogen bubbles, (d) a hydrogen bubble generating circuit consisting of an electronic equipment box, (e) two halogen lamps which were used as light sources at both sides of the wall of the test section area, (f) a circulating pump of submersible pump type, which was submerged in the major tank to supply water to the minor tank, (g) a flow meter which was used to adjust the water flow rate that was supplied to the minor tank, and (h) a still picture camera and a video camera which were used to view and record the motion of the hydrogen bubbles at the top of the test section area.

Figure 4. Experiment setup of flow visualisation by hydrogen bubble technique

Results and Discussion

Numerical results

To study the airflow around the school building and the natural ventilation for classrooms, a number of planes were used to determine the numerical results as displayed in Figure 5. A horizontal plane A and 3 vertical planes B-1, B-2, B-3 display the velocity fields. A vertical lane C is used to study air velocity magnitude around building before blowing through the windows of the three classrooms. Wind that enters through the door is not suitable to ventilate the room because it can blow directly from the floor to the occupants [20]. So the study of airflow around corridor is not considered in this study..

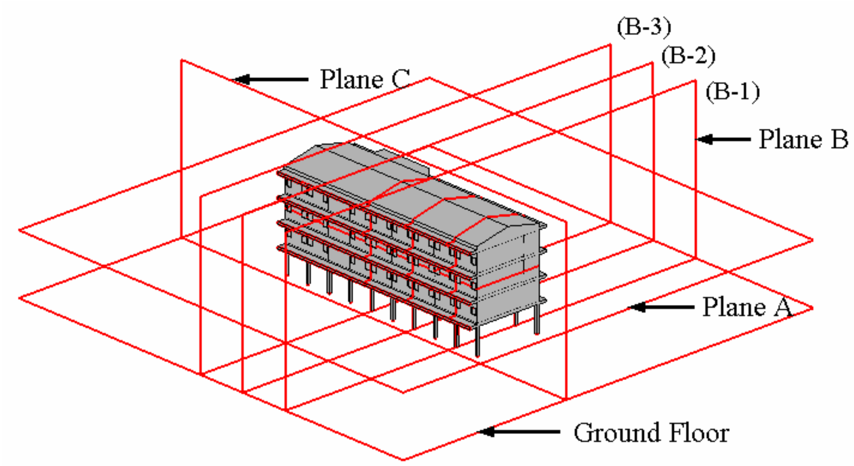

Figure 5. Sliced planes of numerical results. The planes B-1, B-2 and B-3 are sliced at x = 4.10, 12.15, and 20.15 m respectively

Figures 6(a-f) show the horizontal plane of the velocity components at middle height of the 3rd floor according to plane A. The wind that blew parallel to the building had no significant effect on the indoor air flow. Diagonal wind at 15°-60° created a swirl flow in the classrooms while straight wind attacked on the exterior wall, a stagnant flow region being generated around there. High strength wind of 30°-90° WIA tended to flow through the windows of classroom A. At 75° WIA, the wind that passed through the windows of classrooms A and B was straighter than that through classroom C. On the other hand, at 90° WIA classroom C obtained straight wind through the windows. This may have been caused by the location of classroom C which is at the middle of building. In the case of WIA > 90°, it was found that the mirror angle cases of z-axis, i.e. 0° & 180°, 15° & 165°, 30° & 150°, etc., gave no different results. A re-attachment flow, i.e. a separate flow found to the left sharp edge of the building and reattaching itself to the building, occurred at left end of the corridor. The flow next to the re-attachment tended to remain in the direction of the main upstream. Stagnant flow was found around the façade. A small area of stagnant zone was found at 15° WIA as shown in Figure 6(a). This zone expanded gradually and became largest at 90°. This type of zone of recirculation flow might form one of the contaminated regions [21].

Figures 7(a-f) show the vertical plane of the velocity components at the middle of the three classrooms (A, B and C) according to planes B-1, B-2, and B-3, respectively. At 90° WIA, it was found that the main flows tended to go up above the roof or down under the basement rather than fully going straight to the building wall at the 3rd floor. This is known as the downwash-upwash pattern on the upwind wall. A velocity field of higher speed wind curves upward over the roof and decelerates as it curves downward over the wake on the downwind side of the façade. The downwind wall of the building exhibits a region of low average velocity and high turbulence [21]. The upward flow was found to exist over most of the façade. The rooms on the 4th floor received a diagonal wind in an upward direction through the windows. On the other hand, the rooms on the 2nd floor received a downward wind. A stagnant flow was found around the exterior wall of the 3rd floor. A similar behaviour of wind blow was also found with the WIA at 270°. Numerical results of 90° and 270° WIA were similar. A zone of recirculating flow was found behind the leeward wall. These numerical results are consistent with those recommended by Tantasavasdi et al. [5], that the elevated floor allows more wind to flow to the building. On the other hand, an on-slab design essentially creates a reverse flow at the façade, reducing the natural ventilation rate.

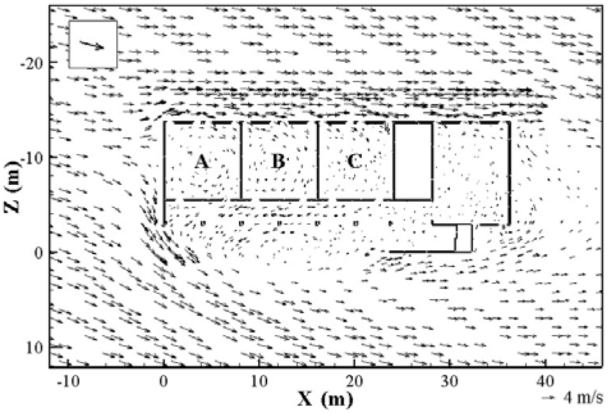

(a) 15°

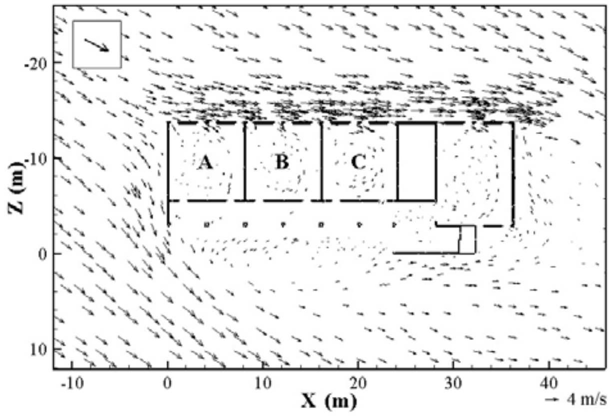

(b) 30°

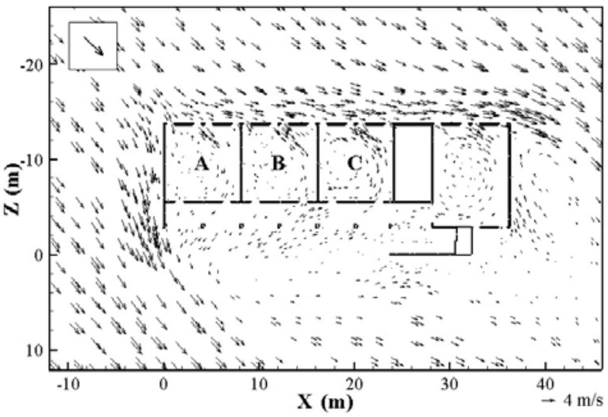

(c) 45°

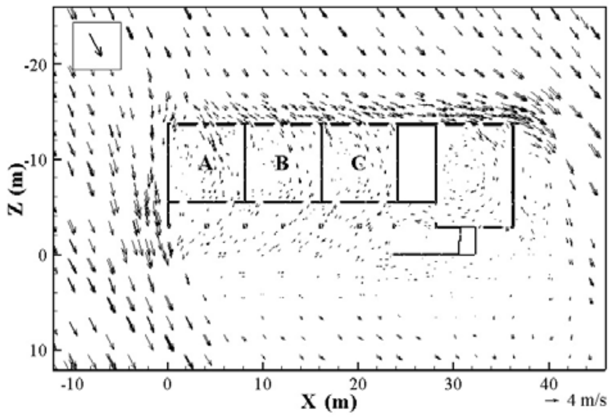

(d) 60°

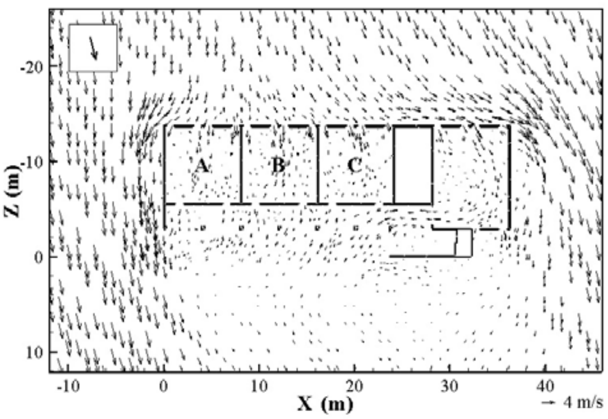

(e) 75°

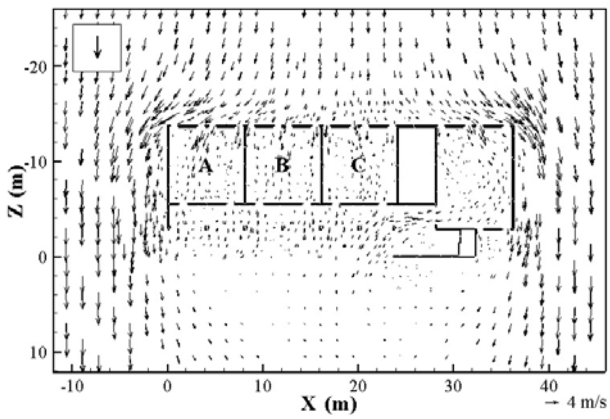

(f) 90°

Figure 6. Horizontal velocity fields on the 3rd floor: Figures (a-f) correspond to WIA = 15°, 30°, 45°, 60°, 75°, and 90° respectively.

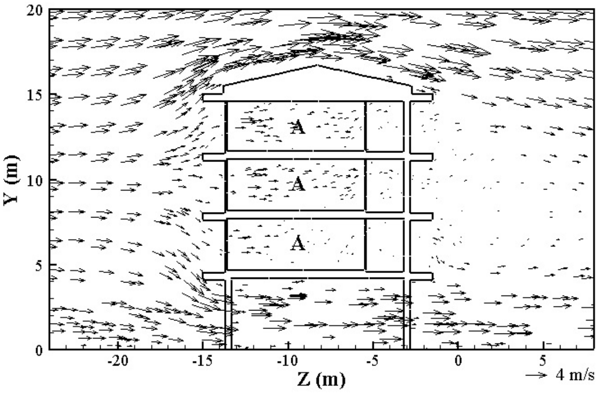

(a) 90° (B-1)

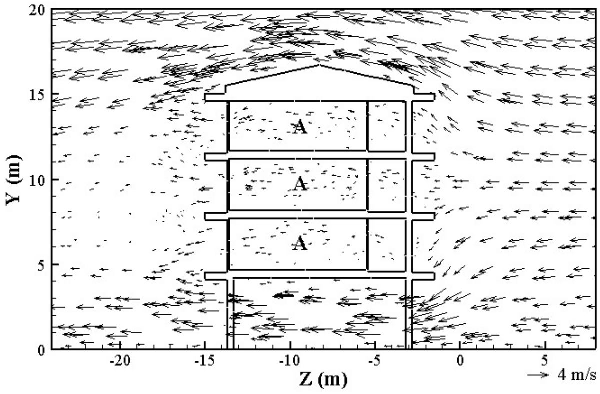

(b) 270° (B-1)

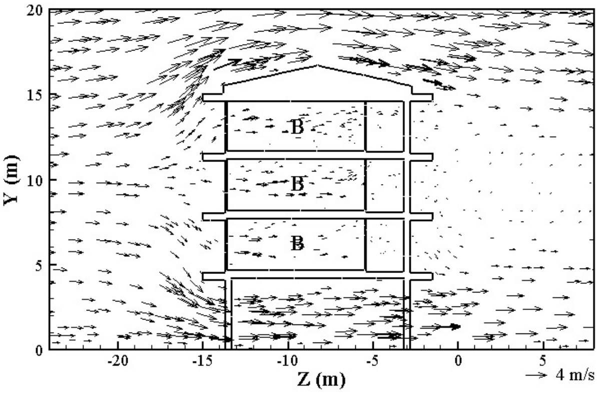

(c) 90° (B-2)

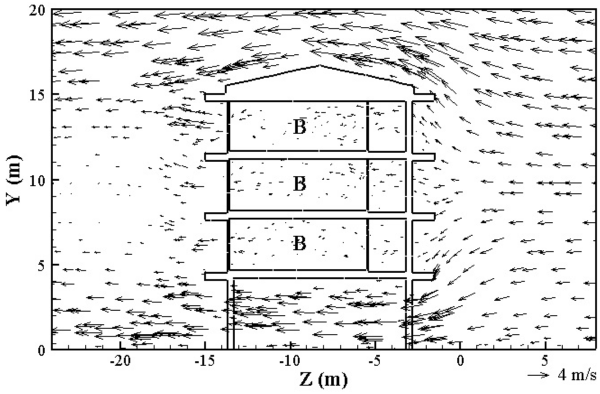

(d) 270° (B-2)

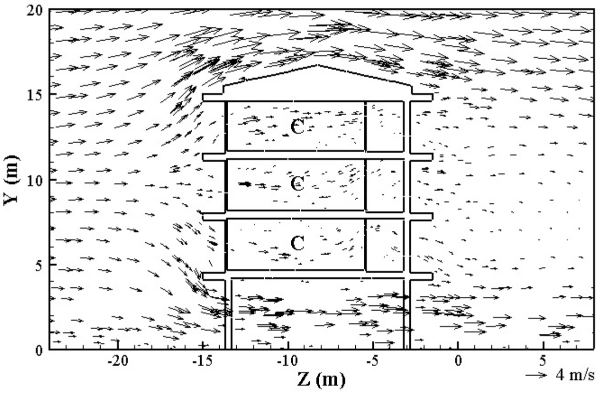

(e) 90° (B-3)

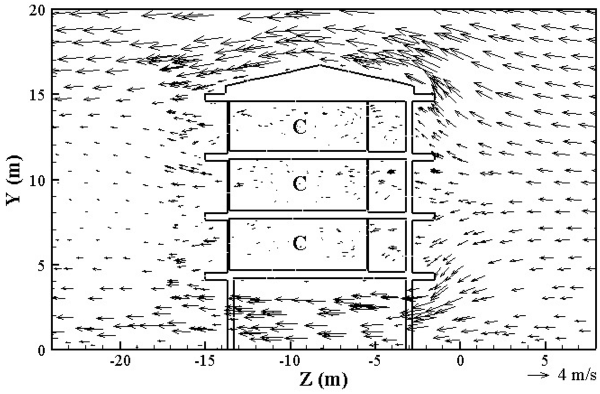

(f) 270° (B-3)

Figure 7. Vertical velocity fields at the middle of the classrooms: The planes B-1, B-2, and B-3 are sliced at x = 4.10, 12.15, and 20.15 m respectively.

From Figures 8(a-f), according to plane C in Figure 5, which is sliced at z = -15 m, it was found that the wind velocity around the window openings of classroom B was same as the classroom C but different from classroom A, especially when WIA increased to 90°. This may be attributed to the corner position of building. Therefore classroom A was not included in this study. The 90° WIA case showed that the wind velocity magnitude around the window openings was less than at other WIAs, i.e. a stagnant zone was found around the window side wall. The wind that blew down to the basement floor had a greater magnitude than that to the upper floors. Wind speeds and directions before passing through the windows of all classrooms (B and C) were averaged and shown in Table 1. From the arithmetic mean value of wind velocity, it was found that the mirror angle cases of z-axis were similar (0° & 180°, 15° & 165° and 30° & 150°). Wind speed was reduced before reaching the boundary of the building, and its direction changed while it approached the building. Hence the horizontal angle was found to differ from WIA significantly, a direct impingement case. The incoming wind speeds and directions will be used as the inlet boundary conditions for the classroom computational domain in future work. It would be useful to develop and plan a natural ventilation strategy in the building orientation for classrooms. This may improve thermal comfort of the students. Local meteorological data, e.g. wind speed, wind direction and ambient temperature may be collected and utilised with the findings from this study to identify an appropriate window opening. Appropriate location, type and size of the window may be investigated to obtain better ventilation.

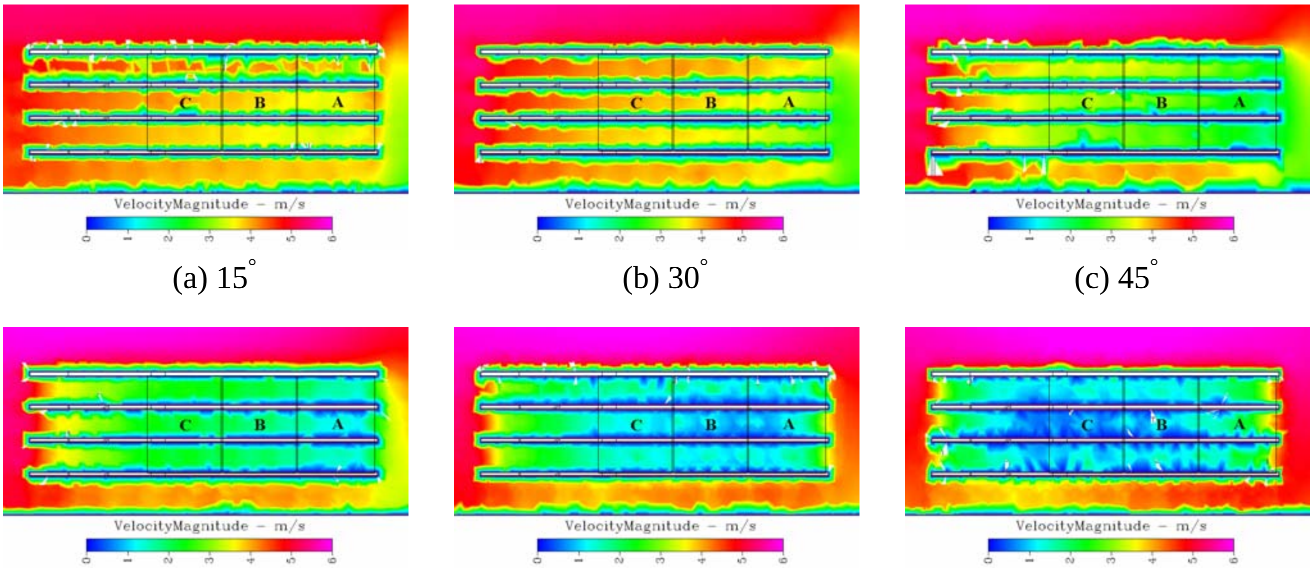

(a) 15° (b) 30° (c) 45°

(d) 60° (e) 75° (f) 90°

Figure 8. Wind velocity magnitudes adjacent to exterior wall: Figures (a-f) correspond to WIA = 15°, 30°, 45°, 60°, 75°, and 90° respectively.

Table 1. Average wind speed and direction in classrooms B and C

WIA (degree)	Velocity magnitude (m/s)[a]	Horizontal angle (degree)[b]
0	1.43/0.37 (1.14-2.01)	2.14
15	2.83/0.14 (2.64-2.96)	3.92
30	2.96/0.27 (2.69-3.35)	6.39
45	2.10/0.19 (1.73-2.25)	11.29
60	1.72/0.18 (1.46-1.98)	20.33
75	0.97/0.13 (0.75-1.10)	48.94
90	0.76/0.21 (0.42-1.01)	109.98 (-70.02)

[a] Arithmetic mean/Standard deviation (range)

[b] Relative to x-axis according to Fig. 3; minus sign denotes mirror direction.

Experimental results

A flow visualisation by hydrogen bubble technique was conducted to support the numerical results visually. A building model (made of plywood) with a scale of 1:500 was placed in the test section area of the water channel. A dimensional analysis was undertaken to determine the water flow in the channel. A similarity between the external flow for the school building and that for the building model was calculated based on the Reynolds number. In this experiment it was assumed that the hydrogen bubbles was moved at the same velocity as water [11]. It was difficult to generate hydrogen bubbles by varying the water flow rate because hydrogen bubbles can dissolve in the water rapidly. Therefore an appropriate flow rate of generating hydrogen bubbles had to be maintained. It was easier to vary the flow rate in the simulation. In the first case, a similarity in water flow was determined to simulate a new computational 30° WIA case that was taken to compare with the horizontal cross section. The new computation with wind speed of 3.0 m/s and 30° WIA was modeled for the same Reynolds number. Figure 9 shows a picture from the post-processing of the computational result and a photograph of the experiment in comparison. Similar to the first case, the computational result of a new run with wind speed of 3.0 m/s and 90° WIA was also compared with the vertical cross section. Figure 10 exhibits a side view of the school building in the 90° WIA case. The computed and the experimental results were found to be qualitatively in good agreement.

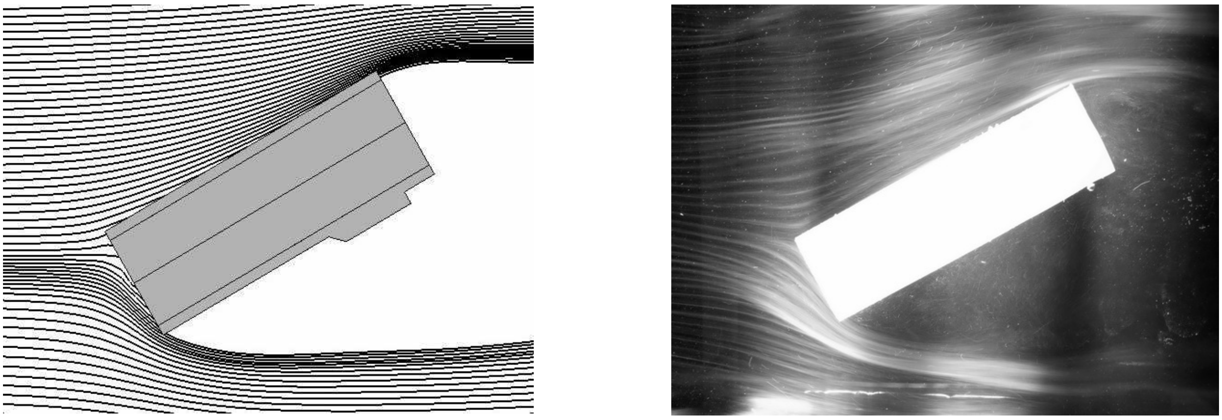

(a) Computational (b) Experimental

Figure 9. Top views of school building models at 30° WIA

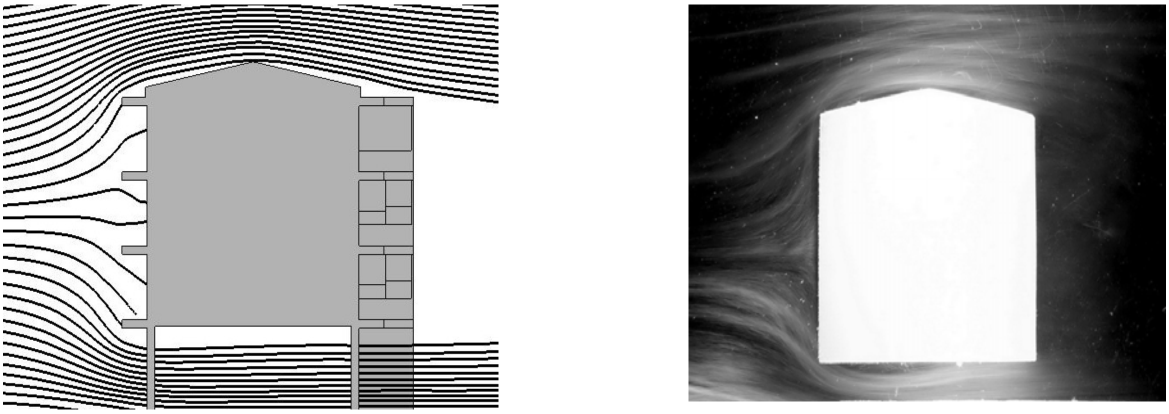

(a) Computational (b) Experimental

Figure 10. Side views of school building models at 90° WIA

Conclusions

An investigation of the airflow around the building of a typical state school which was designed for natural cross-flow ventilation for classrooms was carried out. A three-dimensional CFD program was used as the tool for simulation experiments. The flow around the school building was simulated to obtain the speeds and directions of the circulating wind. Based on the findings, the following conclusions can be drawn:

- The cross orientation of the building to the wind direction may not necessarily result in good ventilation in the classrooms.
- The geometry and orientation of the building has a strong effect to the airflow around it. The rooms in the middle zone of the building seem to get more uniform ventilation than those at the end.
- The flow visualisation by hydrogen bubble technique can give rise to the flow field. This proves to be a useful tool for verifying the numerical results qualitatively.

Acknowledgement

A support from the National Science and Technology Development Agency (Thailand) is highly appreciated.

References

1. L. Yang, G. Zhang, Y. Li, and Y. Chen, "Investigating potential of natural driving forces for ventilation in four major cities in China", *Energy and Buildings*, **2005**, *40*, 738-746.
2. A. Mochida, H. Yoshino, T. Takeda, T. Kakegawa, and S. Miyauchi, "Methods for controlling airflow in and around a building under cross-ventilation to improve indoor thermal comfort", *Journal of Wind Engineering and Industrial Aerodynamics*, **2005**, *93*, 437-449.
3. E. Prianto and P. Depecker, "Optimization of architectural design elements in tropical humid region with thermal comfort approach", *Energy and Buildings*, **2003**, *35*, 273-280.
4. E. Prianto and P. Depecker, "Characteristic of airflow as the effect of balcony, opening design and internal division on indoor velocity", *Energy and Buildings*, **2002**, *34*, 401-409.
5. C. Tantasvasdi, J. Srebric, and Q. Chen, "Natural ventilation design for houses in Thailand", *Energy and Buildings*, **2001**, *33*, 815-824.
6. A. Sreshthaputra, J. Haberl, and M. J. Andrews, "Improving building design and operation of a Thai Buddhist temple", *Energy and Buildings*, **2004**, *36*, 481-494.
7. A. Mochida, H. Yoshino, T. Takeda, T. Kakegawa, and S. Miyauchi, "Methods for controlling airflow in and around a building under cross-ventilation to improve indoor thermal comfort", *Journal of Wind Engineering and Industrial Aerodynamics*, **2005**, *93*, 437-449.
8. G. Evola and V. Popov, "Computational analysis of wind driven natural ventilation in buildings", *Energy and Buildings*, **2006**, *38*, 491-501.
9. C. R. Smith and R. D. Paxson, "A Technique for evaluation of three-dimensional behavior in turbulent boundary layers using computer augmented hydrogen bubble-wire flow visualization", *Experiments in Fluids*, **1983**, *1*, 43-49.
10. C. R. Smith and L. J. Lu, "Image processing of hydrogen bubble flow visualization for determination of turbulence statistics and bursting characteristics", *Experiments in Fluids*, **1985**, *3*, 349-356.
11. S. Eiamsa-ard, C. Leksongneon, S. Sripattanapipat, V. Kongkaitpaiboon, and P. Promvonge, "Visualization study of flow pattern around two obstacles near a channel wall with hydrogen bubble technique", *Proceedings of the 17th Conference of Mechanical Engineering Network of Thailand*, **2003**, TF 026.
12. F. Bao and U. Dallmann, "Some physical aspects of separation bubble on a rounded backward-facing step", *Aerospace Science and Technology*, **2004**, *8*, 83-91.
13. H. Guo, Q. X. Lian, Y. Li, and H. W. Wang, "A visual study on complex flow structures and flow breakdown in a boundary layer transition", *Experiments in Fluids*, **2004**, *37*, 311-322.
14. P. F. Zhang, J. J. Wang, S. F. Lu, and J. Mi, "Aerodynamic characteristics of a square cylinder with a rod in a staggered arrangement", *Experiments in Fluids*, **2005**, *38*, 494-502.
15. CFD Research Corporation, "Engineering Simulations Software", Huntsville, Alabama, **2003**.

16. B. E. Launder and D. B. Spaulding, “The numerical computation of turbulent flows”, *Computational Methods for Applied Mechanical Engineering*, **1974**, *3*, 269-289.
17. J. D. Posner, C. R. Buchanan, and D. Dunn-Rankin, “Measurement and prediction of indoor air flow in a model room”, *Energy and Buildings*, **2003**, *35*, 515-526.
18. C. Nitatwichit, Y. Khunatorn, and N. Tippayawong, “Investigation and characterization of cross ventilation flows through openings in a school classroom”, *Journal of the Chinese Institute of Engineers*, **2008** (in press).
19. G. Gan, “Numerical method for a full assessment of indoor thermal comfort”, *Indoor Air*, **1994**, *4*, 154-168.
20. C. Nitatwichit, Y. Khunatorn, C. Tantakitti, and N. Tippayawong, “Effects of wind speed and incoming direction on indoor airflow pattern in a classroom”, *International Conference on Technology and Innovation for Sustainable Development*, 25-26 January **2006**, Khon Kaen, Thailand.
21. American Society of Heating, Refrigerating and Air-Conditioning Engineers (ASHRAE) Fundamentals Handbook, “Airflow around Buildings”, Atlanta, **2001**, Ch. 16.